Electronic Supplementary Material (ESI) for Analyst.

Supporting information for:

X-ray Diffraction to Probe the Kinetics of Ice Recrystallization Inhibition

Alice Fayter,[a], Steven Huband,[c] Matthew I. Gibson[*],[a,b]

[a] Department of Chemistry, University of Warwick, Coventry, CV4 7AL, United Kingdom

[b] Warwick Medical School, University of Warwick, Coventry, CV4 7AL, United Kingdom

[c] Department of Physics, University of Warwick, Coventry, CV4 7AL, United Kingdom

CORRESPONDING AUTHOR DETAILS

E-mail: m.i.gibson@warwick.ac.uk

Materials

Poly(ethylene glycol) (PEG) (4kDa) and poly(vinyl alcohol) (PVA) (10 kDa), lysozyme and ampicillin were purchased from Sigma-Aldrich and used as supplied unless otherwise stated. Imidazole (Merck) and glycerol (Fisher Chemical), isopropyl-β-D-thiogalactoside (IPTG) (VWR chemical), safranine-O and phenosafranin (ACROS organics), Novex AP Chromogenic and SYTO-9 (Invitrogen) and Coomassie blue stain (Expedeon) were also used as supplied. AFGP8 CC-86-XVII was kindly provided by A. L. DeVries and used as received. Gold nanoparticles were synthesised as reported previously.[1] For washing of AuNPs, Amicon Ultra-0.5 centrifugal filter units with Ultracel-30 membrane were used. 40 nm citrate-stabilised gold colloid solution was purchased from BBI solutions. The pET20b-AFPIII plasmid encoding for a hexahistidine-tagged AFPIII from ocean pout (*rQAE isoform*, M1.1HISPET20b) was kindly provided by Peter Davies (Queens University, Kingston, Canada). Competent *Escherichia coli* BL21(DE3) cells were sourced from New England Biolabs. . IMAC Sepharise 6 Fast Flow columns, HiLoad 16/600 Superdex 75 pg gel filtration columns and PD10 desalting columns were purchased from GE Healthcare and used according to manufacturer's instructions.

Analytical Methods

^{1}H, ^{13}C and ^{19}F-NMR spectra were obtained using a Bruker DPX-400 NMR Spectrometer. Mass spectrometry was carried out in pure methanol or water on the Agilent 6130B ESI-Quad instrument using electrospray in positive mode. FTIR spectroscopy was carried out on a Bruker Vector 22 FTIR spectrometer with a Golden gate diamond attenuated total reflection cell. SEC (GPC) measurements were carried out on an Agilent 390-LC MDS instrument equipped with a dual angle light scatter

(LS), 2 x PLgel Mixed D columns (300 x 7.5 mm) and a PLgel 5 µm guard column. The eluent was DMF with 5 mmol NH_4BF_4 additive. Samples were run at 1ml/min at 50. Poly(methyl methacrylate) standards (Agilent EasyVials) were used for calibration between 955,000 – 550 $gmol^{-1}$. Analyte samples were filtered through a nylon membrane with 0.22 μm pore size before injection. Respectively, experimental molar mass ($Mn,_{SEC}$) and dispersity ($Đ$) values of synthesized polymers were determined by conventional calibration and universal calibration using Agilent GPC/SEC software. Nanoparticle size was determined using Dynamic Light Scattering (DLS), performed on a Malvern Instruments Zetasizer Nano- ZS with 4mW HeNe laser 632.8 nm. UV/Vis spectroscopy, optical density and fluorescence plate readings were performed on a BioTek Synergy HT Microplate Reader. UV-vis spectroscopy was used to determine nanoparticle size according to a method developed by Haiss et al.[2] Transmission electron microscopy (TEM) was performed on a JEOL 2100 LaB6 high-resolution microscope. X-ray photoelectron spectroscopy (XPS) was carried out on the Kratos Axis Ultra with a delay-line detector. Bacterial cell lysis was performed using a STANSTED 'Pressure Cell' FPG12800 homogenizer. XRD experiments were performed using a Xenocs Xeuss 2.0 equipped with a micro-focus Cu K_α source collimated with Scatterless slits. The scattering was measured using a Pilatus 300k detector with a pixel size of 0.172 mm x 0.172 mm. The distance between the detector and the sample was calibrated using silver behenate ($AgC_{22}H_{43}O_2$), giving a value of 0.161(3) m. The detector was fixed at an angle of 36° giving a 2θ range of 18.5 to 47.5°. Samples were mounted in 1.0 mm quartz capillaries (Capillary Tube Supplies Ltd).

Synthetic and Experimental Procedures

Recombinant expression of His-AFPIII

A pET20b-AFPIII plasmid encoding for a hexahistidine-tagged AFPIII from ocean pout (*rQAE isoform*, M1.1HISPET20b) was kindly provided by Peter Davies (Queens University, Kingston, Canada). The plasmid was transformed into competent Escherichia coli BL21(DE3) cells (New England Biolabs). A colony was selected to inoculate 50 mL of LB-medium containing 100 μg/mL ampicillin and was grown overnight at 37 °C under continuous shaking of 180 rpm. The following day, 5 mL of the preculture was added to 500 mL of LB-medium in a 2 L Erlenmeyer flask and grown at 37 °C with a shaking speed of 180 rpm till an OD600 of 0.6 was reached. The temperature was then reduced to 16 °C and IPTG was added to a final concentration of 0.4 mM. The overexpression of the protein was allowed to take place overnight following which the cells were centrifuged at 4000 g for 30 minutes at 4 °C.

Pelleted cells were resuspended in PBS supplemented with Pierce protease inhibitor mini-tablets. The suspension was passed through a STANSTED 'Pressure Cell' FPG12800 homogeniser in order to lyse the cells. The cell lysate was centrifuged at 14,000 g and the supernatant was passed through a 0.45 nm filter and applied to an IMAC Sepharose 6 Fast Flow (GE Healthcare) column charged with Ni(II) ions and pre-equilibrated with PBS. The column was washed with 20 column volumes of 20 mM imidazole in PBS. Bound AFPIII was eluted using 300 mM Imidazole in PBS. The AFPIII was further purified using a HiLoad 16/600 Superdex 75 pg gel filtration column (GE Healthcare) with PBS as the running buffer. Fractions exclusively containing the AFPIII were pooled and concentrated to 5 mg/mL. Purity was estimated using SDS-PAGE and protein concentration determined using Thermo Scientific Pierce BCA assay kit. This was verified by measuring absorbance at 280 nm and obtaining

protein's extinction coefficient [as predicted by ProtParam (http://web.expasy.org/protparam/)] for use in Beer-Lambert law.

Recombinant expression of SNAP-AFPIII

A genetic fragment encoding for AFPIII fused to a hexahistidine tag was amplified from the pET20b-AFPIII plasmid using 5'-GTACGGATCCAACCAGGCTAGCGTTGTG-3' (BamHI site underlined) as the forward primer and 5'-ATTAGCGGCCGCAGCCGGATCTCAGTG-3' (NotI site underlined) as the reverse primer. The BamHI/NotI digested products were ligated into a pSNAP-tag® (T7)-2 vector (New England Biolabs). The plasmid was then transformed into competent Escherichia coli BL21(DE3) cells (New England Biolabs). The subsequent expression and purification was performed as detailed for AFPIII.

General Synthesis of AFP@Au_4 (from Ni-NTA-$pHEA_{17}$-, Maleimide-$pHEA_{47}$- or BG-$pHEA_{45}$@Au_4)

Ni-NTA-$pHEA_{17}$-, Maleimide-$pHEA_{47}$- or BG-$pHEA_{45}$@Au_4 solution (500 μL) was concentrated by centrifugation in Amicon Ultra-0.5 centrifugal filter units with an Ultracel-30 membrane. SNAP-AFP was conjugated to the BG-$pHEA_{45}$@Au_4; Cys-AFP was conjugated to Mal-$pHEA_{47}$@Au_4; and His-AFP was conjugated to Ni-NTA-$pHEA_{17}$@Au_4. To this concentrate was added the same volume of protein solution as was originally concentrated to retain the same concentration of AuNPs. This was left, agitating, for 120 minutes at room temperature. The solutions were concentrated by centrifugation in Amicon Ultra-0.5 centrifugal filter units with an Ultracel-30 membrane, before being re-dispersed in the same volume of pH 7.5 PBS buffer. The nanoparticles were washed in this manner a further 2 times before being re-dispersed in the same final volume of PBS and stored in the fridge until required. Nanoparticle

size and dispersity was measured by TEM, UV-Vis spectroscopy and size and zeta potential measurements by DLS.

Ice Recrystallization Inhibitory activity splat assay

The sample was prepared in PBS solution, and a 10 μL was dropped onto a glass microscope coverslip atop an aluminium plate cooled to -78 with dry ice. The thin wafer of ice that forms upon contact with the coverslip was transferred to a cryostage held at -8 ºC using liquid nitrogen, and left to anneal for 30 minutes at this temperature. Three images were taken at different locations on this wafer at 20 x zoom under cross polarizers. Using ImageJ, the number of crystals in the images were counted and the average crystal size per wafer was calculated as mean grain area (MGS) as well as the mean grain length size (MLGS).

Modified Sucrose Sandwich Ice Shaping Assay

Samples dissolved in PBS buffer containing 45% sucrose were sandwiched between two glass coverslips and sealed with immersion oil. Samples were cooled to −50 °C on a Linkam Biological Cryostage BCS196 with T95-Linkpad system controller equipped with a LNP95-Liquid nitrogen cooling pump, using liquid nitrogen as the coolant (Linkam Scientific Instruments UK, Surrey, U.K.). The temperature was then increased to −8 °C and held for 1 hour to anneal. The samples were then heated at 0.5 °C.min^{-1} until few ice crystals remained and then cooled at 0.05 °C.min^{-1} and the shape of ice crystals observed. Micrographs were obtained every 0.1 °C using an Olympus CX41 microscope equipped with a UIS-2 20x/0.45/∞/0−2/FN22 lens (Olympus Ltd., Southend on sea, U.K.) and a Canon EOS 500D SLR digital. Image processing was conducted using ImageJ.

X-ray Diffraction Orientation Analysis

Samples were prepared in PBS solution as stated before and 10 μL was inserted into 1 mm thick quartz capillaries and mounted in a Linkam THMS350 furnace and cooled to -35 °C at 30 °C.min^{-1}. The samples were then heated to -8 °C where X-ray scattering was performed. Measurements were made with a counting time of 10 seconds repeatedly, with a 4 second delay between each acquisition, over 1800 seconds annealing, to enable analysis of the number of crystal orientations observed over time and comparison to splat assay data. A radial integration of the 2D scattering profile was performed using FOXTROT 3.3.4 software resulting in 1D intensity versus 2θ plots. In addition, azimuthal integrations for each Bragg peak were performed producing 1D intensity versus ψ plots. Data was then ran through an in-house MATLAB programme to obtain the number of ice crystal orientations. Each data point with an intensity greater than a threshold value 1.5 counts) was counted as a crystal orientation. The total number of data points (#orientations) was calculated for a 1D intensity versus ψ file using the following line of code:

```
NumberOfOrientations{i}=sum(Intensities{i}>IntensityThreshold);
```

This was run in a script calculate the number of orientations for each Bragg peak and to handle the large number of datasets produced in the annealing studies. To compare the rate of crystal growth the gradient of change in orientations over time was obtained.

Supplementary Figures

To further exemplify the use of this method, gold-nanoparticle (AuNP) conjugated AFPs which we have previously reported were also investigated;[1] Figure S1. IRI activity was studied for AFPIII upon conjugation to AuNP via two linkers and the XRD method compared to traditional microscopy. The number of crystal orientations were obtained and show broad agreement with MLGS data, showing that this XRD method also works for complex materials. His-AFP and SNAP-AFP are both IRI active, and at the concentrations shown they both give mean largest grain length values between 20-30% that of a PBS control. Once bound to gold nanoparticles the IRI-activity of SNAP-AFP is only slightly affected; MLGS change of 4%. However, for His-AFP there is a reduction of 68% giving a result close to that of a PBS control, Figure S1A/B. These results are mirrored in the WAXS orientation analysis; for ice doped His-AFP@Au, the number of crystal orientations greatly decreases; and for SNAP-AFP@Au, where the IRI-activity is retained, the number of orientations decreases minimally, Figure S1C.

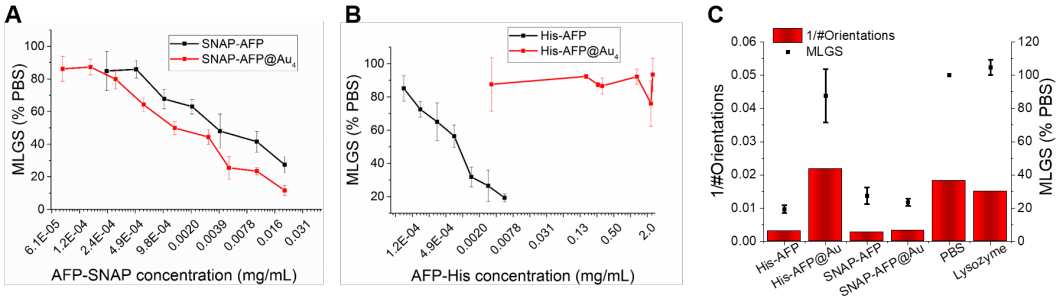

Figure S1: Splat assay data for AFPIII unbound and bound to AuNP using two different tags; A) SNAP-tag; B) His-tag, prepared in PBS; C) Comparison of orientation analysis (here shown as inverse number of observed ice crystal orientations after 1800 seconds) and IRI-activity (shown as mean length grain size, MLGS, as a percentage of PBS) for His-AFP and SNAP-AFP bound and unbound to AuNP. [Lysozyme] = 0.7 $mg.mL^{-1}$, [AFPIII-His] = 0.4 $mg.m^{-1}$, [AFPIII-SNAP] = 0.1 $mg.mL^{-1}$, [AFGP8] = 0.07 $mg.mL^{-1}$.

The relative rates obtained from XRD for ice crystal growth for IRI active compounds compared to that of their respective negative controls over a range of concentrations are shown in Figures S2, S3 and S4.

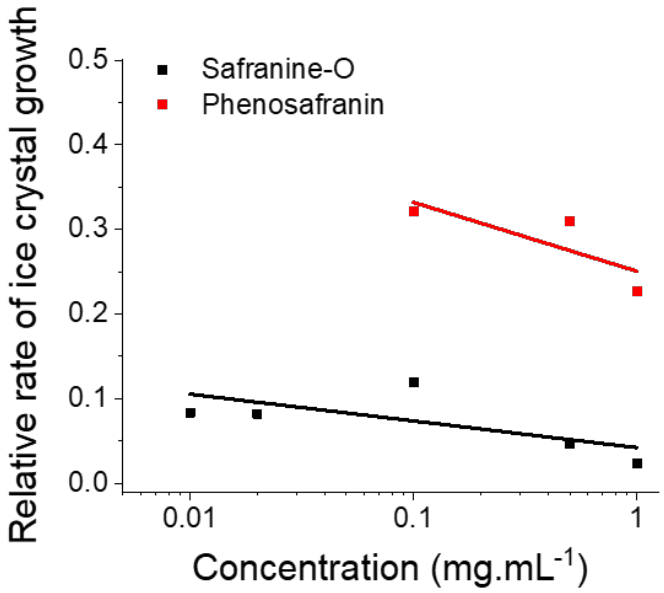

Figure S2. Relative ice growth rates compared to that of ice crystal growth for pure water for a range of concentrations; safranine-O (black) and phenosafranin (red) after 1800 seconds annealing at -8 °C.

As the concentration of IRI active compound increases, the calculated gradient of initial change in number of crystal orientations gradually tends towards zero, from an increase in 0.007 crystals/s to 0.002 crystals/s, (Figure S2). The rate for inactive phenosafranin also decreases but is up to 10x faster than that of safranine-O, with an average increase of 0.026 crystals/s.

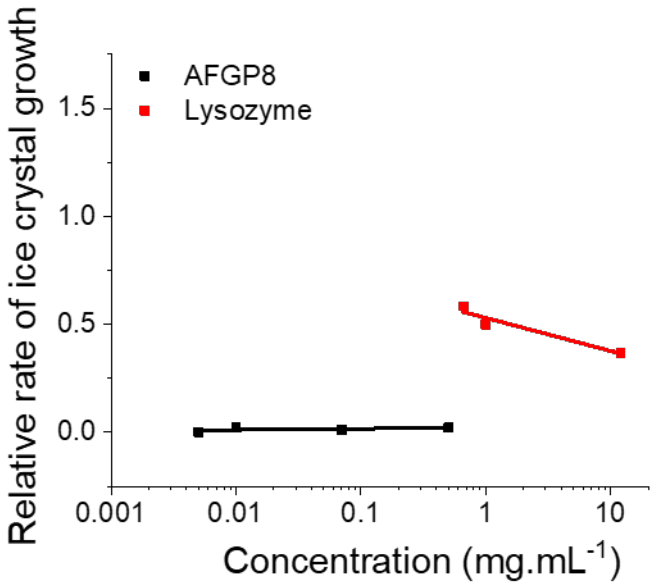

Figure S3. Relative ice growth rates compared to that of ice crystal growth for pure water for a range of concentrations of AFGP8 (black) and lysozyme (red) after 1800 seconds annealing at -8 °C.

For the concentrations of AFGP8 studied here (Figure S3), the mean rate of change in ice crystal orientations does not change – this is because AFGP8 is extremely active, even at low concentrations (lowest concentration tested here was 0.005 $mg.mL^{-1}$). The average rate for all concentrations is 0.00125 crystals/s, which is much lower than that of the lysozyme control, which is 0.041 crystals/s. 3 concentrations of lysozyme, an IRI-inactive protein were tested and the initial rate of change in number of crystal orientations barely differed; even between concentrations of 1 and 12 $mg.mL^{-1}$, with rates of 0.042 and 0.031 crystals/s respectively, thus lysozyme decreases in number of orientations therefore has fewer, but larger ice crystals after the 1800 s anneal. The mean rate for the samples was found to be 0.041 and was compared to all AF(G)P samples tested.

Limitations of technique

This method does not give the actual number of ice crystals, but rather the number of orientations in the polynucleated samples, which is proportional to the number of crystals. Under-determination of number of crystals could be an issue if the crystallites are sufficiently small and the number of orientations very large (when the number of grains is large enough that diffraction occurs at all ψ angles), resulting in the measured intensity being above the threshold value at every data point. This would put a limit on the maximum number of orientations that can be determined as the total number of data points in the azimuthal integrations. This is not an issue in the samples tested here but it is important to highlight that evaluation with an optical method in parallel is still required. This limit is equipment dependant and could be improved by increasing the sample to detector distance or by using a detector with a reduced pixel size.

References

1. Wilkins, L. E., Hasan, M., Fayter, A. E. R., Walker, M. & Gibson, M. I. Site-specific conjugation of antifreeze proteins onto polymer-stabilized nanoparticles. *Polym. Chem.* (2019). doi:10.1039/c8py01719k

2. Haiss, W., Thanh, N. T. K., Aveyard, J. & Fernig, D. G. Determination of Size and Concentration of Gold Nanoparticles from UV - Vis Spectra. *Anal. Chem.* **79**, 4215–4221 (2007).

3. Mitchell, D. E. *et al.* Ice-recrystallization inhibiting polymers protect proteins against freeze-stress and enable glycerol-free cryostorage. *Mater. Horizons* (2019). doi:10.1039/C8MH00727F

4. Hasan, M., Fayter, A. E. R. & Gibson, M. I. Ice Recrystallization Inhibiting Polymers Enable Glycerol-Free Cryopreservation of Micro-organisms. *Biomacromolecules* **19**, 3371–3376 (2018).